Disruption of the SucT acyltransferase in *Mycobacterium smegmatis* abrogates succinylation of cell envelope polysaccharides

Received for publication, March 22, 2019, and in revised form, May 14, 2019 Published, Papers in Press, May 20, 2019, DOI 10.1074/jbc.RA119.008585

Zuzana Palčeková[‡], Shiva K. Angala[‡], Juan Manuel Belardinelli[‡], Haig A. Eskandarian[§], Maju Joe[¶], Richard Brunton[¶], Christopher Rithner[‖], Victoria Jones[‡], Jérôme Nigou[**], Todd L. Lowary[¶], Martine Gilleron[**], Michael McNeil[‡], and Mary Jackson[‡1]

*From the [‡]Mycobacteria Research Laboratories, Department of Microbiology, Immunology, and Pathology, Colorado State University, Fort Collins, Colorado 80523-1682, the [§]Global Health Institute, Ecole Polytechnique Fédérale de Lausanne, 1015 Lausanne VD, Switzerland, the [¶]Alberta Glycomics Centre and Department of Chemistry, University of Alberta, Edmonton, Alberta T6G 2G2, Canada, the [‖]Central Instrumentation Facility, Department of Chemistry, Colorado State University, Fort Collins, Colorado 80523-1872, and the **Institut de Pharmacologie et de Biologie Structurale, Université de Toulouse, CNRS, UPS, 205 Route de Narbonne, 31077 Toulouse, France*

Edited by Gerald W. Hart

Similar to other prokaryotes, mycobacteria decorate their major cell envelope glycans with minor covalent substituents whose biological significance remains largely unknown. We report on the discovery of a mycobacterial enzyme, named here SucT, that adds succinyl groups to the arabinan domains of both arabinogalactan (AG) and lipoarabinomannan (LAM). Disruption of the SucT-encoding gene in *Mycobacterium smegmatis* abolished AG and LAM succinylation and altered the hydrophobicity and rigidity of the cell envelope of the bacilli without significantly altering AG and LAM biosynthesis. The changes in the cell surface properties of the mutant were consistent with earlier reports of transposon mutants of the closely related species *Mycobacterium marinum* and *Mycobacterium avium* harboring insertions in the orthologous gene whose ability to microaggregate and form biofilms were altered. Our findings point to an important role of SucT-mediated AG and LAM succinylation in modulating the cell surface properties of mycobacteria.

Covalent modification of cell envelope glycans with strategically placed discrete substituents such as various sugars, amino acids, phosphates, or acyl groups is a common strategy used by prokaryotes to adapt and survive under various stress conditions, including the environment of the infected host. Although not required for growth *per se*, these tailoring modifications may affect the biosynthesis, export, and/or biological activities of polysaccharides, thereby impacting the cell envelope composition and physical properties of the bacteria, their resistance to antimicrobials, and their interactions with host immune responses (1–9). A classic example of how such modifications may thwart host defenses is masking by Gram-negative and Gram-positive bacteria of the negative charges conferred by the phosphate groups of lipopolysaccharide, wall teichoic acids, and lipoteichoic acids with positively charged amines under the form of amino sugars, phosphoethanolamine, or D-alanyl esters to evade killing by positively charged antimicrobial peptides. Although devoid of the canonical lipopolysaccharide and (lipo)teichoic acids, mycobacteria produce polysaccharides and lipopolysaccharides with unique structures that play critical roles in their cell envelope integrity and pathogenicity (10–11). The finding of covalent substituents modifying the structures of two of the dominant heteropolysaccharides produced by all *Mycobacterium* species, arabinogalactan (AG)[2] and lipoarabinomannan (LAM), suggests that mycobacteria have evolved similar strategies as other prokaryotes to promote their survival in different environments (12). To date, however, our understanding of the biological significance of these discrete substituents is, at best, rudimentary.

The arabinan domain of LAM is very similar to that of AG and made of stretches of α-1,5–linked arabinofuranosyl (Ara*f*) residues with precisely positioned α-3,5 branch sites (Fig. 1). In *Mycobacterium tuberculosis* and a number of other slow- and fast-growing pathogenic mycobacteria (*Mycobacterium avium*, *Mycobacterium kansasii*, *Mycobacterium bovis*, *Mycobacterium leprae*, and *Mycobacterium abscessus*), the C2 position of a portion of the internal α-3,5–branched Ara*f* residues of the arabinan domain of AG may be modified with galactosamine substituents, a motif not found in LAM (13) (Fig. 1). Studies from our laboratory have shed light on the biosynthetic origin of this substituent (13) and begun to elucidate its contribution to modulation of the host immune response (14). Interestingly,

This work was supported by NIAID, National Institutes of Health Grant AI064798 (to M. J.) and the Alberta Glycomics Centre (to T. L. L.). The authors declare that they have no conflicts of interest with the contents of this article. The content is solely the responsibility of the authors and does not necessarily represent the official views of the National Institutes of Health.

This article contains Figs. S1–S10, Tables S1–S4, and Supporting Methods.

[1] To whom correspondence should be addressed. Tel.: 970-491-3582; Fax: 970-491-1815; E-mail: Mary.Jackson@colostate.edu.

[2] The abbreviations used are: AG, arabinogalactan; LAM, lipoarabinomannan; AM, D-arabino-D-mannan; LM, lipomannan; mAGP, mycolyl–AG–peptidoglycan; OADC, oleic acid–albumin–dextrose–catalase; ADC, albumin–dextrose–catalase; Tricine, *N*-[2-hydroxy-1,1-bis(hydroxymethyl)ethyl] glycine; AFM, atomic force microscopy; HMQC, heteronuclear multiple quantum coherence; TS, tryptic soy.

© 2019 Palčeková et al. Published under exclusive license by The American Society for Biochemistry and Molecular Biology, Inc.

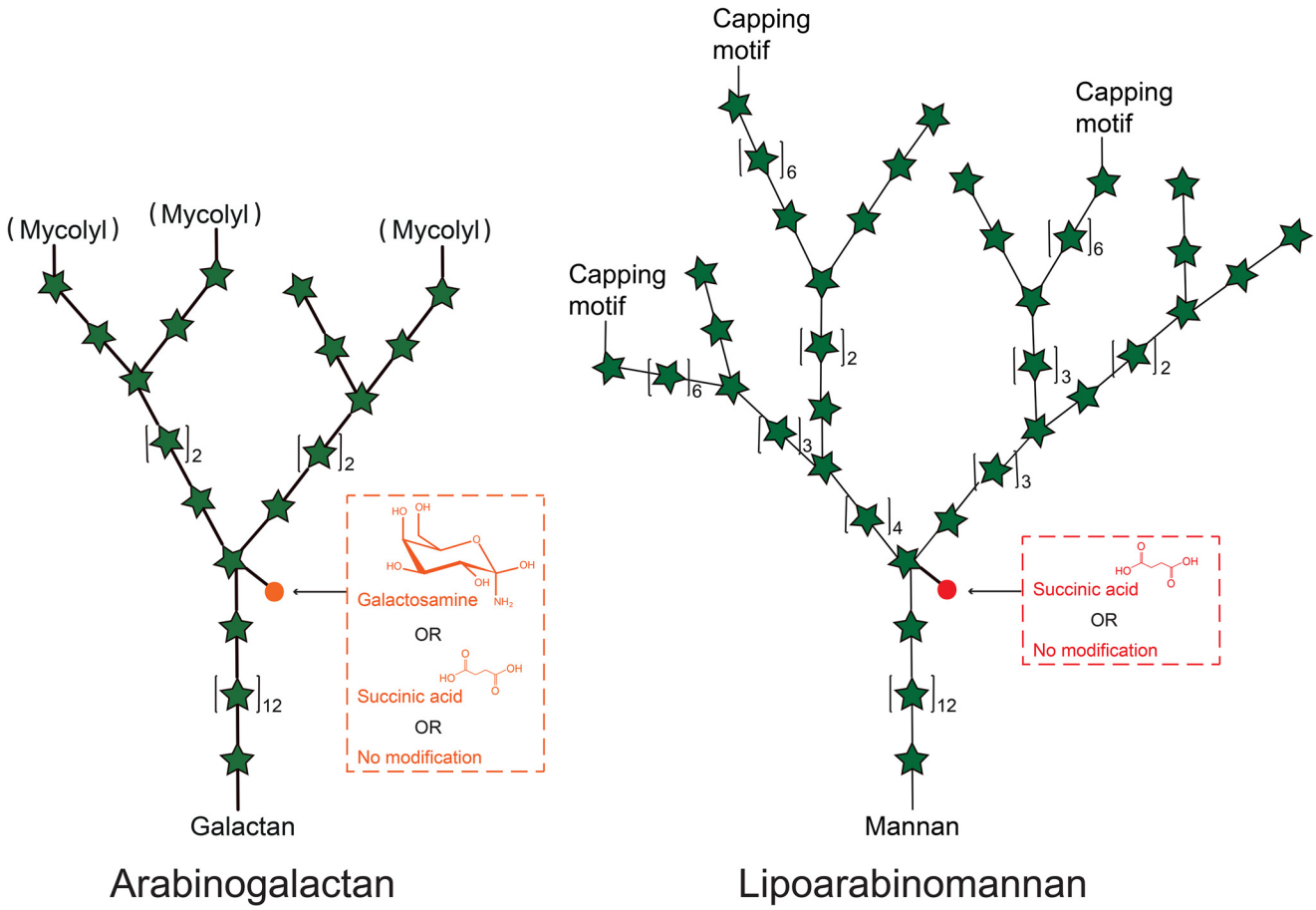

Figure 1. Detail of the chemical modifications affecting the internal arabinan domains of AG and LAM in *M. tuberculosis*. Note that the succinylation of the mycolylated chains in arabinogalactan has been reported to be diminished or absent (15).

succinate groups were found to substitute the same positions of the arabinan domain as well as quantitatively minor α-1,5-Ara*f* positions of AG from *M. tuberculosis* and *Mycobacterium smegmatis* (15), the internal α-3,5–branched Ara*f* residues of the arabinan domain of LAM from *M. bovis* Bacillus Calmette-Guerin (BCG) (16), and possibly the same positions of LAM from *M. leprae* and *M. tuberculosis* (17–21). The presence of succinates has also been reported on the capsular polysaccharide D-arabino-D-mannan (AM) of *M. tuberculosis*, which shares with LAM a structurally identical arabinomannan domain (22). Succinates were finally found to substitute the C3 position of linear α-1,5–Ara*f* residues of LAM in *M. kansasii* (23). Collectively, these observations are suggestive of the widespread distribution of succinate motifs in the AG and LAM of mycobacteria, even though their precise position on these glycans may be variable from species to species. Succinyl substituents were estimated to occur at the level of about one to three motifs per arabinan chain in AG, one to six motifs per LAM molecule, and two to three motifs per AM molecule (15–17, 22). Neither the enzyme(s) catalyzing the introduction of these motifs in the arabinan domain of AG, AM, and LAM nor the precise biological significance of polysaccharide succinylation in mycobacteria are currently known, even though an association was suggested between the charge of various LAM isoforms (in part driven by succinate content) and their ability to stimulate CD1b-restricted T cells (19, 21). It has further been proposed that the negatively charged succinyl residues interact with the protonated galactosamine substituents, leading to a more rigid and tightened AG structure (15). Assuming that succinates are introduced during elongation of the arabinan domains of AG and LAM, these motifs could also serve as molecular signatures regulating elongation and branching (12). Alternatively, the apparent lack of succinylation on the mycolylated arabinan chains of AG (Fig. 1) has led to the hypothesis that succinylation negatively controls mycolylation (15).

Here we report the identification of a conserved mycobacterial acyltransferase, hereafter referred to as SucT, responsible for the succinylation of AG and LAM and the significant impact of disruption of *sucT* on the physiology of *M. smegmatis* cells. The possibility of generating mycobacterial mutants deficient in succinylation of cell envelope polysaccharides paves the way for studies aiming to determine the contribution of this discrete substituent to the physiology of slow- and fast-growing mycobacteria, their adaptation to the environment, and immunopathogenesis.

Results

Identification of a candidate enzyme for succinylation of AG and LAM

A bioinformatics search for protein candidates with potential for catalyzing the succinylation of the arabinan domains of AG

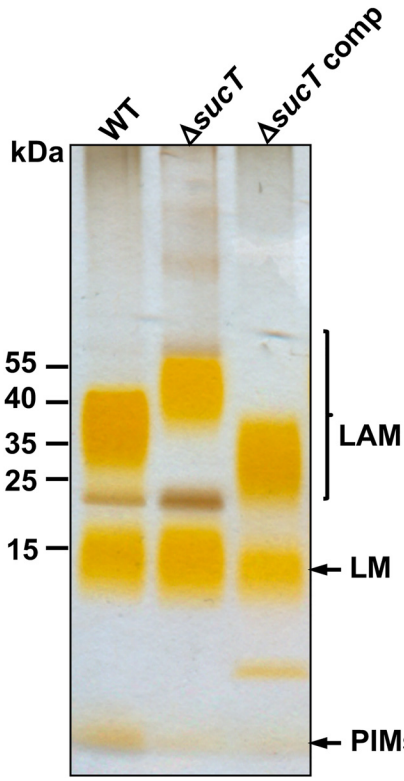

Figure 2. Electrophoretic mobility of lipoglycans from WT *M. smegmatis* mc²155, the *sucT* mutant, and the complemented *sucT* mutant. Lipoglycans extracted from WT mc²155, mc²Δ*sucT*, and mc²Δ*sucT*/pMVGH1-*sucT* (Δ*sucT comp*) were run on a 10–20% Tricine gel, followed by periodic acid–silver staining. *PIMs*, phosphatidylinositol mannosides.

and LAM identified five integral membrane proteins (Rv0111, Rv0228, Rv0517, Rv1254, and Rv1565c) in *M. tuberculosis* and nine homologous proteins in *M. smegmatis* (MSMEG_0206, MSMEG_0319, MSMEG_0390, MSMEG_2021, MSMEG_3187, MSMEG_3490, MSMEG_5041, MSMEG_5537, and MSMEG_6230) showing sequence similarities with a family of trans-acylases (COG1835) involved in *O*-acylation of exported carbohydrate moieties in a variety of prokaryotes. Enzymes from this family include a number of O antigen, exopolysaccharide, and Nod factor acetyltransferases as well as macrolide acyltransferases (24). In line with the prototypical primary and secondary structures of these enzymes, all five *M. tuberculosis* candidate acyltransferases harbor nine to ten transmembrane segments and display conserved cytoplasmic and transmembrane amino acid residues reported to be critical for activity (24–26) (Fig. S1). All *M. tuberculosis* candidates are conserved in mycobacteria, with the exception of Rv0517, which is partially or completely deleted in some *M. tuberculosis* clinical isolates and is apparently missing from *M. leprae*. While TmaT (Rv0228 in *M. tuberculosis* and MSMEG_0319 in *M. smegmatis*) was recently shown to acetylate mycolic acids (27–28), other candidates have not yet been functionally characterized.

Given the presence of succinate motifs on the AG and LAM of *M. smegmatis* (15, 17, 20), individual KOs of each conserved candidate gene with clear orthologs in *M. tuberculosis* were generated by allelic replacement in this nonpathogenic, fast-growing model species (Fig. S2*A*), and their lipoglycans were analyzed by SDS-PAGE. As shown in Fig. 2 and Fig. S2*B*, the *MSMEG_3187* mutant (orthologous to *Rv1565c* of *M. tuberculosis*) was the only one to present a lipoglycan profile significantly different from that of the WT parent strain. Although its lipomannan (LM) migrated similarly to that of the WT strain, its LAM migrated higher, suggestive of alterations in either size or charge (Fig. 2). Complementation of the *MSMEG_3187* KO with a replicative plasmid expressing a WT copy of the *MSMEG_3187* gene expressed from the *hsp60* promoter reversed the slow migration of LAM on SDS-PAGE beyond WT levels. MSMEG_3187 shares 23% identity (40% similarity) on a 705-amino acid overlap with the O antigen acetyltransferase OafA from *Salmonella* (24). We renamed this protein SucT for the purpose of this study.

Disruption of sucT results in loss of succinyl substituents on the LAM of M. smegmatis

To determine whether a defect in succinylation and, thus, overall charge of the *sucT* mutant LAM might be responsible for its migration shift on SDS-PAGE, LAM was purified from the WT, *sucT* KO (*Msmg*Δ*sucT*), and complemented mutant strain (*Msmg*Δ*sucT*/pMVGH1-*sucT*) and submitted to a panel of analyses. Direct analysis of succinyl groups was performed by butanolysis of LAM prepared from the WT, mutant, and complemented mutant strains to yield dibutyl esters of any succinyl groups present (Supporting Methods). GC/MS analysis revealed a complete absence of succinates in the mutant LAM. LAM succinylation was restored beyond WT levels in the complemented mutant. Quantitation of the ratio of succinyl to arabinosyl groups showed a ratio of 1:9.5 (S.D. ± 0.4 for two determinations) for the WT strain and 1:6 (S.D. ± 0.1 for three determinations) following ectopic overexpression of *MSMEG_3187* in *Msmg*Δ*sucT*/pMVGH1-*sucT* (Fig. 3*A*).

Next, LAM prepared from each of the three strains was analyzed for the presence of succinates by 1D and 2D NMR spectroscopy (16). The 1D ^{1}H spectrum of LAM prepared from the WT strain showed the characteristic two pseudotriplets (J = 6.5 Hz) of similar intensities at 2.50 and 2.66 ppm (Fig. 4*A*) assigned to methylene groups of succinyl units. Their corresponding carbons were characterized at 34.7 and 33.3 ppm, respectively, on the 2D ^{1}H-^{13}C HMQC spectrum (Fig. 4*B*). The cross-peaks between ^{1}H δ 4.96/^{13}C δ 81.9 and ^{1}H δ 4.94/^{13}C δ 82.1 further typify the presence of succinyl residues on the C2 of α-3,5–branched Ara*f* residues and, possibly, some adjacent α-1,5–Ara*f* residues (16). These signals were absent from the 1D ^{1}H and 2D HMQC spectra of the mutant LAM (Fig. 4, *C* and *D*) and restored upon genetic complementation Fig. 4, *E* and *F*). Collectively, our analyses support the conclusions that succinates substitute α-3,5–branched Ara*f* residues of the arabinan domain of LAM in *M. smegmatis*, as reported previously in *M. bovis* BCG (16), and that the *M. smegmatis sucT* KO is devoid of any such substituents.

Because of the report of succinates on the LM of an unspecified *M. smegmatis* strain (20), we next sought to verify whether the succinylation defect extended to the mutant's LM. Comparison of the WT and mutant LM by NMR spectroscopy, however, failed to identify any succinates on the LM of the *M. smegmatis* mc²155 parent strain used in this study (Fig. S3). Overall,

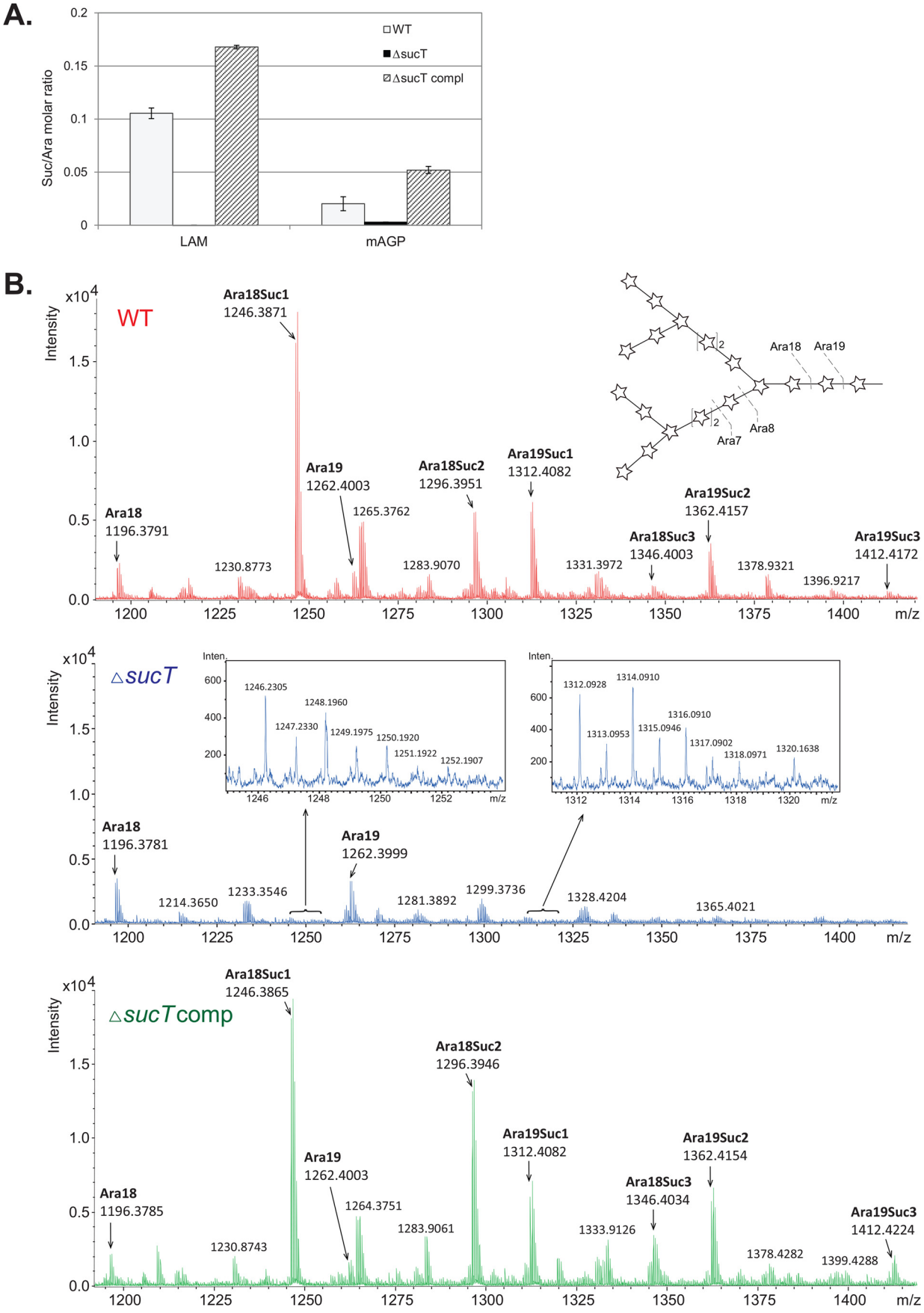
A.
Suc/Ara molar ratio
0.2
0.15
0.1
0.05
0
WT
ΔsucT
ΔsucT compl
LAM
mAGP
B.
WT
Intensity
x10^4
Ara18Suc1
1246.3871
Ara19
1262.4003
Ara18Suc2
1296.3951
Ara19Suc1
1312.4082
Ara18
1196.3791
1265.3762
Ara19Suc2
1362.4157
Ara18Suc3
1346.4003
Ara19Suc3
1412.4172
1230.8773
1283.9070
1331.3972
1378.9321
1396.9217
Ara18
Ara19
Ara8
Ara7
m/z
ΔsucT
Inten.
1246.2305
1248.1960
1247.2330
1249.1975
1250.1920
1251.1922
1252.1907
1312.0928
1314.0910
1316.0910
1313.0953
1315.0946
1317.0902
1318.0971
1320.1638
Ara18
1196.3781
Ara19
1262.3999
1214.3650
1233.3546
1281.3892
1299.3736
1328.4204
1365.4021
ΔsucTcomp
Ara18Suc1
1246.3865
Ara18Suc2
1296.3946
Ara19Suc1
1312.4082
Ara19Suc2
1362.4154
Ara18Suc3
1346.4034
Ara19Suc3
1412.4224
Ara18
1196.3785
Ara19
1262.4003
1264.3751
1283.9061
1230.8743
1333.9126
1378.4282
1399.4288

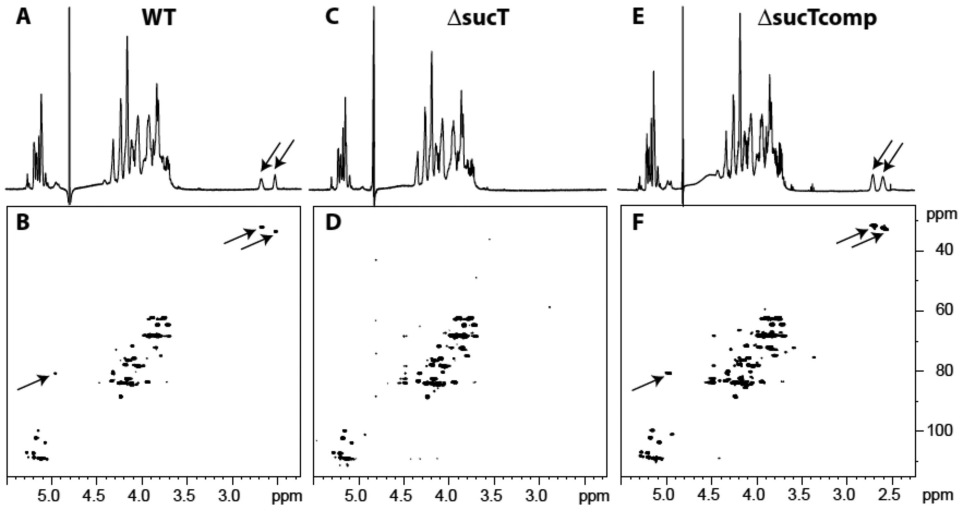

Figure 4. NMR analysis of LAM prepared from the WT, mutant, and complemented mutant strains. Shown are 1D ^{1}H (*A*, *C*, and *E*) and 2D ^{1}H-^{13}C (*B*, *D*, and *F*) HMQC NMR spectra. *Arrows* point to the signals typifying succinate detection and localization (see text for details).

no significant structural differences were noted between the LM prepared from *Msmg*Δ*sucT* and the WT strain.

Interestingly, a screen for *Mycobacterium marinum* transposon mutants devoid of mannose caps on LAM yielded a strain harboring a transposon insertion in *MMAR_2380*, the ortholog of *sucT* in this species (75% identity/85% similarity at the protein level with MSMEG_3187) (29). Not only was this mutant confirmed to lack mannoside caps on LAM, it also displayed a higher degree of branching of both the mannan core and the arabinan domain compared with WT LAM and decreased acylation of the phosphatidylinositol anchor of both LM and LAM. In contrast to the *M. marinum MMAR_2380* mutant, *Msmg*Δ*sucT* failed to show any reduction in the incorporation of [1,2-^{14}C]acetate into the acyl chains of LM and LAM (Fig. S4*A*). Likewise, quantitative analyses of the alditol acetate and per-*O*-methylated alditol acetate derivatives of the WT, mutant, and complemented mutant LAM did not point to any significant alterations in the Ara*f* to Man*p* ratio of the mutant LAM (Table S1) or increase in the degree of branching of its mannan and arabinan domains (Table S2). The relative proportion of Ara_4 to Ara_6 arabinan termini of LAM was also similar in the WT and mutant strains (relative percentage of Ara_2, Ara_4, and Ara_6 oligoarabinosides released upon *Cellulomonas gelida* endoarabinanase digestion: 58.7% ± 4.6%, 37.5% ± 5.2%, and 3.8% ± 0.7%, respectively, in the WT strain compared with 60.9% ± 3.4%, 34.3% ± 4.3%, and 4.8% ± 1.0% in the *sucT* mutant; average ± S.D. of three technical replicates). ^{31}P NMR and LC/MS analysis of the oligoarabinosides released upon *C. gelida* endoarabinanase digestion of deacylated LAM further confirmed the presence of the expected phosphoinositol capping motifs of *M. smegmatis* LAM in the WT and mutant strains (Fig. S5, *A* and *B*). Metabolic labeling of WT and mutant cultures with [^{14}C]glucose finally pointed to similar rates of *de novo* lipoglycan synthesis in both strains (Fig. S4*B*). Collectively, these results suggest that, besides abolishing succinylation, the disruption of *sucT* did not appreciably affect, either qualitatively or quantitatively, the biosynthesis of LAM in *M. smegmatis*.

Effect of inactivating sucT on the succinylation of M. smegmatis AG

Given the structural similarity of the arabinan domains of AG and LAM, we next sought to determine whether the disruption of *sucT* had any impact on the succinate content of AG from *M. smegmatis*. To this end, the mycolyl–AG–peptidoglycan (mAGP) complex prepared from the WT, mutant, and complemented mutant strains was subjected to the same butanolysis procedure as for LAM, and succinyl substituents as their dibutyl esters were analyzed by GC/MS. Compared with the WT parent, mAGP from the *sucT* KO showed an 84.7% decrease in succinate content. Quantitation of the ratio of succinyl to arabinosyl groups yielded a ratio of 1:52 (S.D. ± 14.3 for three determinations) for the WT strain, 1:350 (S.D. ± 20.9 for two determinations) for *Msmg*Δ*sucT*, and 1:19 (S.D. ± 1.2 for three determinations) for *Msmg*Δ*sucT*/pMVGH1-*sucT* (Fig. 3*A*). To gain further insight into the degree of succinylation of AG in the different strains, their mAGP was digested with endogenous *M. smegmatis* endoarabinanase, and the released oligoarabinosides were analyzed by LC/MS as described in the Supporting Methods. The mass spectra of the arabinans released from the WT and complemented mutant AG revealed nonsuccinylated and succinylated Ara_{18} and Ara_{19} oligoarabinosides, whereas only the nonsuccinylated variants were detected in *Msmg*Δ*sucT* (Fig. 3*B*). Similar to the situation with *M. tuberculosis* (15), the fact that Ara_7 fragments showed a significantly (~ 3-fold) smaller degree of succinylation is inter-

Figure 3. Succinate content of AG and LAM prepared from WT *M. smegmatis* mc^{2}155, the Δ*sucT* mutant, and the complemented mutant strain. *A*, the amounts of succinates and arabinose residues in the same LAM and mAGP samples prepared from the WT, mutant, and complemented mutant (Δ*sucT compl*) strains were quantified as described in the Supporting Methods. Results are expressed as average ± S.D. succinate/arabinose molar ratios from three technical replicates. *B*, endogenous endoarabinanase digestion of mAGP from the WT, mutant, and complemented mutant strains. Analysis of the products of the reaction by QTOF LC/MS in the negative ion mode revealed characteristic $[M\text{-}2H]^{-2}$ ions corresponding to oligoarabinosides with succinyl groups in the WT and complemented mutant that are not found in the *sucT* mutant mAGP.

preted as the succinyl residues being located on the interior branched α-3,5–Ara*f* residue. This observation, combined with the fact that Ara_{18} may have up to four succinyl substituents, leads to the identification of quantitively minor positions of succinylation on adjacent linear α-1,5–branched Ara*f* residues (Fig. 3*B*). The fact that *Msmg*Δ*sucT* mAGP was not entirely devoid of succinates, according to the butanolysis analysis, could indicate that succinyl groups substitute, in a SucT-independent manner, other positions of AG not revealed by our LC/MS analysis of oligoarabinosides. Alternatively, because the GC/MS analysis of succinyl substituents was performed on mAGP rather than on purified AG, we cannot exclude that the remaining succinates arose from peptidoglycan and/or mycolic acids.

Analyses of the monosaccharide composition (Table S3) and glycosyl linkages (Table S4) of the WT, mutant, and complemented mutant AG otherwise failed to reveal any significant structural alterations in the galactan or arabinan domains of the mutant AG. The degree of mycolylation of the mutant AG was also similar to that measured in the WT strain (Table S3).

Alterations in the cell surface properties of the sucT mutant

Two previous studies have reported on the isolation and partial characterization of *Mycobacterium* mutants carrying transposon insertions in *sucT* orthologs. First was the study by Driessen *et al.* (29), mentioned above, in which a *M. marinum sucT* KO mutant was identified as part of a screen for strains devoid of mannoside caps on LAM. Second was the screening by Yamazaki *et al.* (30) of an *M. avium* transposon mutant library for strains impaired in biofilm formation, which also yielded a mutant harboring an insertion in *sucT*. Although neither of these studies reported on the function of *sucT* and its impact on succinylation of AG and LAM, interesting observations were made regarding the growth and cell surface properties of the mutants. The *M. marinum* mutant, although displaying WT colony morphology on 7H10 agar plates, was reported to be hyperaggregative in 7H9-ADC-Tween 80 medium (29). The *M. avium sucT* mutant, on the other hand, was found to display an altered colony morphology on agar and to be impaired in its ability to form biofilms on polyvinyl chloride microplates (30). Our observations point to *Msmg*Δ*sucT* sharing characteristics of both the *M. marinum* and *M. avium sucT* transposon mutants in that it aggregated in 7H9-ADC-Tween 80 medium and displayed an altered colony morphology on 7H11-OADC agar (Fig. 5*A*). Monitoring of the absorbance and colony-forming unit counts of *Msmg*Δ*sucT* cultures over time in 7H9-ADC-tyloxapol medium (where satisfactory bacterial dispersion was achieved) also reproducibly pointed to a slight reduction in growth of the mutant compared with the WT strain, marked by an extended lag period (Fig. S6*A*). Despite having recovered the ability to succinylate both AG and LAM and a WT colonial morphology (Fig. 5*A*), the complemented mutant showed a growth rate more comparable with that of the *sucT* KO (Fig. S6*A*), a result that may tentatively be explained by the hyper-succinylation of AG and LAM in this strain. Further analysis revealed that *Msmg*Δ*sucT* was slightly retarded in its ability to form surface biofilm pellicles in Sauton's medium, a phenotype probably resulting (at least in part) from its slower growth. Surface pellicle formation was partially restored upon genetic complementation (Fig. S6*B*).

Because the hyperaggregative properties and biofilm defect of the *M. smegmatis sucT* KO were suggestive of changes in cell surface hydrophobicity, the WT, mutant, and complemented mutant were next compared for their ability to bind the lipophilic dye Congo red (31). In liquid TS broth, *Msmg*Δ*sucT* cells bound more than four times more Congo red than the WT and complemented strains, pointing to a clear increase in cell surface hydrophobicity (Fig. 5*B*). This phenotype also reflected on TS agar supplemented with Congo red, where the WT and complemented mutant strains grew as dry white colonies, whereas the *sucT* KO grew as glossy red colonies (Fig. 5*B*). Drug susceptibility testing further indicated that the *sucT* mutant was eight times more susceptible to rifampicin, a drug thought to penetrate the *M. smegmatis* outer membrane through passive diffusion (Table 1).

To gain further insight into the cell envelope properties of the *sucT* mutant, the surface rigidity of the WT, mutant, and complemented mutant cells in relation to their height was measured using correlated optical fluorescence microscopy and atomic force microscopy. Results pointed to an ~ 1.7-fold increase in the mean surface rigidity of the mutant compared with the WT and complemented mutant strains (Fig. 5*C*).

To investigate the possible reasons underlying the increased hydrophobicity and other surface alterations of the *M. smegmatis sucT* mutant, the surface lipids from this strain were finally extracted and compared with the cell surface lipid contents of the WT and complemented mutant. TLC analyses pointed to the reproducible buildup of three compounds in the *sucT* mutant that were either not detected or present in much lesser quantities at the surface of the WT and complemented strains (Fig. S7*A*). The nature of these products is at present not known, but staining with α-naphthol suggests that they may be glycolipids. TLC analyses of total lipids from the same *M. smegmatis* strains upon metabolic labeling with [1,2-^{14}C]acetate did not reveal any other notable differences between the WT and *sucT* KO (Fig. S7*B*). Likewise, comparative analysis by LC/MS of the contents of the WT and *sucT* mutant in another succinylated lipopolysaccharide, known as the methylglucose lipopolysaccharide, failed to reveal any significant differences between the two strains (Fig. S8).

Discussion

Similar to other mycobacterial species, *M. smegmatis* has been known to acylate its two major cell envelope glycans, AG and LAM, with succinyl groups even though their biological significance and biosynthetic origin have remained elusive. The data presented here show that succinyl substituents precisely modify the C2 position of α-3,5-branched Ara*f* residues of the arabinan domain of LAM in *M. smegmatis* and possibly the same position of the arabinan domain of AG, with the possibility for adjacent linear α-1,5-branched Ara*f* residues to be succinylated as well. Data further show that SucT (MSMEG_3187) is the sole enzyme responsible for this modification in both LAM and AG.

The identification of SucT as the enzyme responsible for the modification of AG and LAM with succinyl groups raises ques-

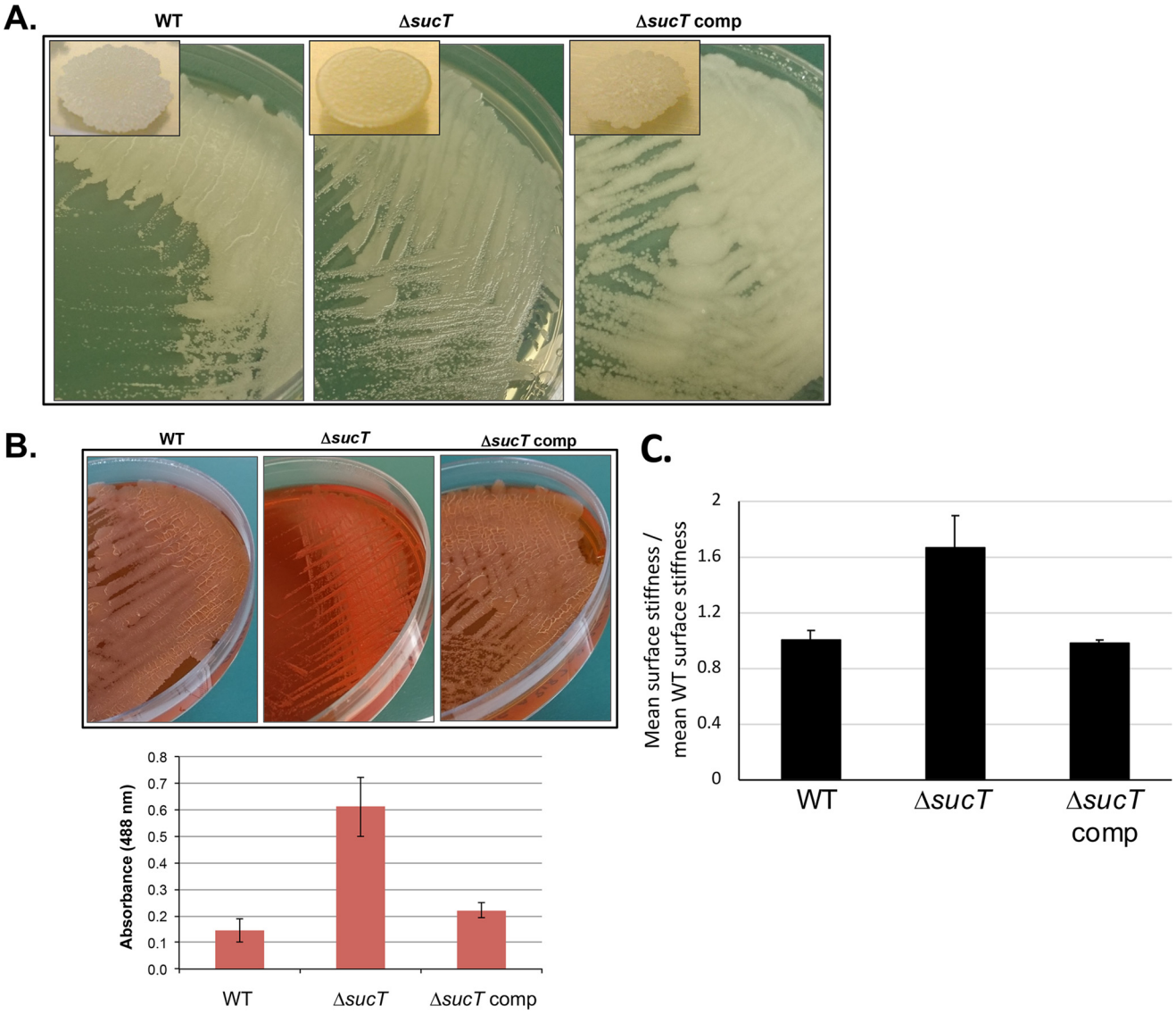

Figure 5. Alterations in the cell surface properties of the *M. smegmatis sucT* mutant. *A*, colony morphology of WT mc^{2}155, mc^{2}Δ*sucT*, and mc^{2}Δ*sucT*/pMVGH1-*sucT* (Δ*sucT comp*) after 3 days of incubation on 7H11-OADC agar at 37 °C. *B*, Congo red binding on a TS agar plate and in TS liquid medium (*graph*). Shown on the graph are the average ± S.D. absorbances of acetone extracts measured for three biological replicates. *C*, analysis of the cell surface rigidity of the WT, mutant, and complemented mutant strains by correlated optical fluorescence and AFM. Two-sided rank sum test demonstrates a statistically significant difference in stiffness between the *sucT* mutant and both the WT ($p = 0.0214$) and the *sucT* complemented mutant ($p = 0.0011$).

Table 1

Susceptibility of the *M. smegmatis sucT* knockout mutant to antibiotics

MIC were determined in 7H9-ADC-tyloxapol and MIC values are in micrograms per milliliter. MIC determinations were performed two to three times on independent culture batches. HYG, hygromycin; KAN, kanamycin; GEN, gentamycin; CIP, ciprofloxacin; INH, isoniazid; EMB, ethambutol; RIF, rifampicin; ND, not determined.

Strains	HYG	KAN	GEN	RIF	INH	CIP	EMB
WT	10	1.2	2.5	50	12.5	0.3	0.8
mc^{2}Δ*sucT*	5–10	1.2	2.5	6.2	12.5	0.15	0.8–1.6
mc^{2}Δ*sucT*/pMVGH1-*sucT*	ND	0.6	ND	50	25	0.3	0.8

tions regarding where and when the introduction of these substituents occurs. Both the arabinan domains of AG and LAM are synthesized on the periplasmic face of the plasma membrane through what appears to be sequential addition of Ara*f* residues by polyprenyl-phosphate-arabinose–dependent arabinosyltransferases (10). It is thus reasonable to assume that the succinylation of AG and LAM takes place on the periplasmic side of the membrane. The mechanism of acyl transfer catalyzed by the family of integral membrane trans-acylases to which SucT belongs, however, has to date not been fully been resolved. The fact that the repeating unit of O-antigen from *Salmonella* Typhimurium is synthesized intracellularly originally led Slauch *et al.* (24) to predict that OafA-like enzymes catalyzed acyl transfer on the cytoplasmic face of the plasma membrane using acyl-CoAs as acyl donors. The rather widespread distribution of functional residues across cytoplasmic loops and transmembrane segments of these enzymes (25–26), however, makes it difficult to precisely map their catalytic site,

raising the possibility that acyl transfer may perhaps occur on the periplasmic side from still unknown high-energy acyl donors. The cytoplasmic succinylation of Ara*f* residues in mycobacteria would entail modification of Ara*f* on the cytoplasmic arabinose donor, polyprenyl-phosphate-arabinose. In light of our failure to detect succinylated polyprenyl-phosphate-arabinose by LC/MS in total lipid fractions from *M. tuberculosis* (data not shown), the hypothesis of periplasmic modification of the arabinan domains of AG and LAM is preferred.

A second important question regarding the catalytic reaction catalyzed by SucT relates to the precise stage in the biosynthesis of AG and LAM at which succinylation occurs. The modification of Ara*f* residues during elongation of the arabinan of AG/LAM could suggest a role of these substituents in governing the elongation and branching of the arabinan domain. Succinylation of AG and LAM upon completion of their synthesis, on the contrary, would rule out their involvement in biosynthesis and rather point to other functions in the physiology of the bacterium and/or its interaction with the host. The conflicting phenotypes of the *M. marinum* and *M. smegmatis sucT* mutants, where the first one displays a significantly altered LAM structure (29) and the second does not, preclude a conclusive answer to this question. It is clear from our results that succinylation is neither critical for biosynthesis of the galactan, mannan, and arabinan domains of AG and LAM nor for the capping of LAM with phosphoinositol caps in *M. smegmatis*. As a first step toward determining whether differences in the LAM biosynthetic pathways of slow- and fast-growing mycobacteria might have accounted for the contrasting phenotypes between the LAM structures of the *M. marinum* and *M. smegmatis sucT* mutants, we tested the ability of the *sucT* gene from *M. tuberculosis* (*Rv1565c*; 83% identity at the amino acid level with MMAR_2380 from *M. marinum* and 75% identity with MSMEG_3187 from *M. smegmatis*) to complement the *M. smegmatis sucT* mutant. The results, which are presented in Fig. S9, point to partial restoration of LAM succinylation in the complemented strain, validating *Rv1565c* as a LAM succinyltransferase. The reason underlying the more critical role of succinylation in elongation and branching of LAM (and perhaps AG) in slow- compared with fast-growing *Mycobacterium* species thus remains to be determined. Unfortunately, our attempts to develop a cell-free assay to determine whether *M. smegmatis* SucT acts on the arabinan domain during its elongation or upon its completion failed to detect any succinyltransferase activity associated with SucT, whatever the enzyme source (*Escherichia coli* lysates expressing *M. smegmatis sucT*, cell-free extracts prepared from *M. smegmatis* WT and the *sucT* KO) or acceptor substrates used: neoglycolipid acceptors mimicking the interior linear and branched structures of the arabinan domain of AG and LAM (Fig. S10) or intact mutant LAM devoid of succinyl substituents (data not shown).

A clear conserved effect of LAM and/or AG succinylation across slow- and fast-growing *Mycobacterium* species, based on reports of *sucT* mutants in *M. avium*, *M. marinum*, and now *M. smegmatis*, is on the cell surface properties of the bacilli (29–30). That these changes in surface properties are the result of alterations in the mycolylation of AG, as proposed earlier (15), was precluded by our analyses of the *M. smegmatis* mutant. Instead, our analyses of the cell surface composition of *MsmgΔsucT* point to an impact of AG and/or LAM succinylation on the production and/or export of some still unknown lipids. The control AG and LAM succinylation has on the bacilli's surface rigidity and hydrophobicity likely has significant implications for the way mycobacteria interact with their environment, including that of the infected host. A defect in biofilm formation, for instance, is expected to negatively impact the ability of mycobacteria to colonize environmental and host substrata as well as their tolerance to biocides. From a virulence standpoint, the *M. avium sucT* KO has been reported to be impaired in its ability to invade bronchial epithelial cells and cause lung infection in mice (32) while replicating similarly as its WT parent in THP-1 human mononuclear phagocytes (33). Whether AG/LAM succinylation contributes similarly to the adaptation of tuberculous mycobacteria to their environment and to immunopathogenesis is currently under investigation in our laboratory.

Experimental procedures

Bacterial strains and growth conditions

M. smegmatis mc^{2}155 was grown under agitation at 37 °C in Middlebrook 7H9 medium supplemented with 10% albumin–dextrose–catalase (ADC) (BD Biosciences) and 0.05% Tween 80 or 0.05% tyloxapol, on Middlebrook 7H11 agar supplemented with 10% oleic acid–albumin–dextrose–catalase (OADC) (BD Biosciences), in glycerol–alanine–salts (GAS) medium with 0.05% tyloxapol, or in Sauton's medium as surface pellicles. Apramycin, kanamycin, hygromycin, and streptomycin were added to final concentrations of 25 μg ml^{-1}, 25 μg ml^{-1}, 50 μg ml^{-1}, and 20 μg ml^{-1}, respectively.

M. smegmatis knockout and complemented knockout mutants

The temperature-sensitive/*sacB* method was used to knock out each of the candidate succinyltransferases of *M. smegmatis* (34). Allelic exchange substrates consisted of an antibiotic cassette (apramycin, streptomycin, kanamycin, or hygromycin) flanked by ~1,000 bp of upstream and downstream homologous DNA sequence flanking *MSMEG_2021*, *MSMEG_3187*, *MSMEG_5041*, *MSMEG_5537*, and *MSMEG_6230*. Primer sequences for these constructs are available upon request. KO mutants were confirmed by PCR using sets of primers located outside of the allelic exchange substrates. For complementation of the *MSMEG_3187* KO, the entire coding sequence of *MSMEG_3187* was PCR-amplified from *M. smegmatis* mc^{2}155 genomic DNA and cloned into the replicative expression plasmid pMVGH1 (35), yielding pMVGH1-*sucT*. pMVGH1-*Rv1565c*, the plasmid used to complement the *MSMEG_3187* KO with the *Rv1565c* gene from *M. tuberculosis*, was PCR-amplified from *M. tuberculosis* H37Rv genomic DNA and similarly cloned into pMVGH1.

Metabolic labeling

Radiolabeling of *M. smegmatis* with [1,2-^{14}C]acetic acid (1 μCi ml^{-1}; specific activity, 52 mCi mmol^{-1}; PerkinElmer Life

Sciences) or [U-^{14}C]glucose (1 μCi ml^{-1}; specific activity, 5 mCi mmol^{-1}; American Radiolabeled Chemicals) was performed in 7H9-ADC-tyloxapol and GAS-tyloxapol, respectively, at 37 °C for 4 h with shaking.

Preparation and analysis of lipids, methylglucose lipopolysaccharides, lipoglycans, and arabinogalactan

Total lipids from *M. smegmatis* cells were extracted with $CHCl_3$/CH_3OH (1:2, v/v) for 2 h at 56 °C, followed by two 2-h extractions with $CHCl_3$/CH_3OH (2:1, v/v) at 56 °C. Surface-exposed lipids were extracted from whole cells in water-saturated 1-butanol as described previously (36), and the butanol-treated cells were then re-extracted twice for 2 h with $CHCl_3$/CH_3OH (2:1, v/v) at 56 °C to recover all remaining extractable lipids. Cold and radiolabeled lipids were analyzed on silica gel 60–precoated TLC plates (F_{254}, Merck) in a variety of solvent systems to resolve lipids of various polarities. TLC plates were revealed by spraying with cupric sulfate (10% w/v in an 8% v/v phosphoric acid solution) or α-naphthol (1% w/v in ethanol) and charring. Radiolabeled products were visualized using a Sapphire Biomolecular Imager (Azure Biosystems).

Methylglucose polysaccharides were extracted from whole cells as described previously (37) and analyzed as described by De *et al.* (38) by ultraperformance LC on a Waters Acquity UPLC H-Class system coupled to a Bruker MaXis Plus quadrupole time-of-flight MS instrument.

Lipoglycan and mAGP complex extraction from delipidated cells followed earlier procedures (15, 39). Lipoglycans were purified by gel exclusion chromatography (40) and analyzed by SDS-PAGE on commercial Novex^{TM} 10–20% Tricine gels stained with periodic acid–Schiff reagent. Other procedures related to the structural analysis of LAM and mAGP are detailed in the Supporting Methods.

Congo red binding

M. smegmatis strains were tested for Congo red binding in TS broth as described by Etienne *et al.* (31). Briefly, the strains were cultivated for 3 days at 37 °C with shaking in TS broth containing 100 μg/ml Congo red. Cells were collected by centrifugation and washed extensively with distilled water until the supernatant was colorless. Cells were next resuspended in 1 ml of acetone, vortexed, and gently shaken for 2 h at room temperature prior to pelleting by centrifugation. Congo red in the supernatants was quantified spectrophotometrically at 488 nm. Congo red binding was defined as the $A_{488\ nm}$ of the acetone extracts divided by the dry weight (in milligrams) of the cell pellet.

Drug susceptibility testing

Minimum inhibitory concentration (MIC) values were determined in 7H9-ADC-tyloxapol in a total volume of 100 μl in 96-well microtiter plates. *M. smegmatis* cultures grown to early log phase ($A_{600\ nm}$ ~0.2) were diluted to a final concentration of 10^6 cfu/ml and incubated in the presence of serial dilutions of the drugs for 2 days at 37 °C. MICs were determined using the resazurin blue test (41).

Correlated optical fluorescence and atomic force microscopy

Preparation conditions and the technical setup for AFM experiments were conducted according to Eskandarian *et al.* (42). Cells of the *M. smegmatis* WT expressing Wag31-GFP were mixed with nonfluorescent *MsmgΔsucT* and deposited on a polydimethylsiloxane-coated coverslip. WT cells were distinguished from *MsmgΔsucT* cells by optical fluorescence microscopy. AFM measurements were made using a Dimension Icon scan head (Bruker) using ScanAsyst fluid cantilevers (Bruker) with a nominal spring constant of 0.7 N m^{-1} in Peak Force quantitative nanomechanical mode at a force setpoint of ~1 nN and typical scan rates of 0.3 Hz. Indentation on the cell surface was estimated to be ~10 nm with a range of ~5 nm in the *z* axis. Height, peak force error, and Derjaguin-Muller-Toporov (DMT) modulus channels were recorded for all scanned images in the trace and retrace directions. Images were processed using Gwyddion (Department of Nanometrology, Czech Metrology Institute; http://gwyddion.net).[3] ImageJ was used for extracting bacterial cell profiles from height and DMT modulus images in a tabular format. A two-sided Wilcoxon rank-sum *U* test was used to analyze the data, with a continuity correction and confidence level of 95% using MatLab. AFM raw data are available at https://figshare.com/s/9dac3d318fceb04653ca.[3]

Author contributions—Z. P., S. K. A., J. M. B., M. Joe, R. B., J. N., T. L. L., M. G., M. M., and M. Jackson conceptualization; Z. P., S. K. A., J. M. B., H. A. E., M. Joe, R. B., C.R ., J. N., T. L. L., and M. G. investigation; Z. P., S. K. A., J. M. B., H. A. E., M. Joe, R. B., C. R., V. J., J. N., T. L. L., M. G., and M. M. methodology; Z. P., J. M. B., H. A. E., C. R., T. L. L., M. G., M. M., and M. Jackson writing-original draft; Z. P., J. M. B., H. A. E., J. N., T. L. L., M. G., M. M., and M. Jackson writing-review and editing; S. K. A., J. M. B., H. A. E., M. G., M. M., and M. Jackson formal analysis; T. L. L. and M. Jackson funding acquisition; M. M. and M. Jackson supervision; M. Jackson project administration.

Acknowledgments—We thank the Integrated Screening Platform of Toulouse (PICT, IBiSA) for providing access to 600 MHz equipment and Dr. Emilie Huc-Claustre for help with the construction of the M. smegmatis MSMEG_5041 knockout mutant.

References

1. Raetz, C. R., Reynolds, C. M., Trent, M. S., and Bishop, R. E. (2007) Lipid A modification systems in Gram-negative bacteria. *Annu. Rev. Biochem.* **76,** 295–329 CrossRef Medline
2. Swoboda, J. G., Campbell, J., Meredith, T. C., and Walker, S. (2010) Wall teichoic acid function, biosynthesis, and inhibition. *ChemBioChem* **11,** 35–45 Medline
3. Brown, S., Xia, G., Luhachack, L. G., Campbell, J., Meredith, T. C., Chen, C., Winstel, V., Gekeler, C., Irazoqui, J. E., Peschel, A., and Walker, S. (2012) Methicillin resistance in *Staphylococcus aureus* requires glycosylated wall teichoic acids. *Proc. Natl. Acad. Sci. U.S.A.* **109,** 18909–18914 CrossRef Medline
4. Needham, B. D., and Trent, M. S. (2013) Fortifying the barrier: the impact of lipid A remodelling on bacterial pathogenesis. *Nat. Rev. Microbiol.* **11,** 467–481 CrossRef Medline

[3] Please note that the JBC is not responsible for the long-term archiving and maintenance of this site or any other third party–hosted site.

5. Whitfield, C., and Trent, M. S. (2014) Biosynthesis and export of bacterial lipopolysaccharides. *Annu. Rev. Biochem.* **83,** 99–128 CrossRef Medline
6. Schneewind, O., and Missiakas, D. (2014) Lipoteichoic acids, phosphate-containing polymers in the envelope of gram-positive bacteria. *J. Bacteriol.* **196,** 1133–1142 CrossRef Medline
7. Maldonado, R. F., Sá-Correia, I., and Valvano, M. A. (2016) Lipopolysaccharide modification in Gram-negative bacteria during chronic infection. *FEMS Microbiol. Rev.* **40,** 480–493 CrossRef Medline
8. Rajagopal, M., and Walker, S. (2017) Envelope structures of Gram-positive bacteria. *Curr. Top. Microbiol. Immunol.* **404,** 1–44 Medline
9. Gerlach, D., Guo, Y., De Castro, C., Kim, S. H., Schlatterer, K., Xu, F. F., Pereira, C., Seeberger, P. H., Ali, S., Codée, J., Sirisarn, W., Schulte, B., Wolz, C., Larsen, J., Molinaro, A., *et al.* (2018) Methicillin-resistant *Staphylococcus aureus* alters cell wall glycosylation to evade immunity. *Nature* **563,** 705–709 CrossRef Medline
10. Angala, S. K., Belardinelli, J. M., Huc-Claustre, E., Wheat, W. H., and Jackson, M. (2014) The cell envelope glycoconjugates of *Mycobacterium tuberculosis*. *Crit. Rev. Biochem. Mol. Biol.* **49,** 361–399 CrossRef Medline
11. Daffé, M., Crick, D. C., and Jackson, M. (2014) Genetics of capsular polysaccharides and cell envelope (glyco)lipids. *Microbiol. Spectr.* **2,** 14 Medline
12. Angala, S. K., Palčeková, Z., Belardinelli, J. M., and Jackson, M. (2018) Covalent modifications of polysaccharides in mycobacteria. *Nat. Chem. Biol.* **14,** 193–198 CrossRef Medline
13. Škovierová, H., Larrouy-Maumus, G., Pham, H., Belanová, M., Barilone, N., Dasgupta, A., Mikusová, K., Gicquel, B., Gilleron, M., Brennan, P. J., Puzo, G., Nigou, J., and Jackson, M. (2010) Biosynthetic origin of the galactosamine substituent of arabinogalactan in *Mycobacterium tuberculosis*. *J. Biol. Chem.* **285,** 41348–41355 CrossRef Medline
14. Wheat, W. H., Dhouib, R., Angala, S. K., Larrouy-Maumus, G., Dobos, K., Nigou, J., Spencer, J. S., and Jackson, M. (2015) The presence of a galactosamine substituent on the arabinogalactan of *Mycobacterium tuberculosis* abrogates full maturation of human peripheral blood monocyte-derived dendritic cells and increases secretion of IL-10. *Tuberculosis* **95,** 476–489 CrossRef Medline
15. Bhamidi, S., Scherman, M. S., Rithner, C. D., Prenni, J. E., Chatterjee, D., Khoo, K.-H., and McNeil, M. R. (2008) The identification and location of succinyl residues and the characterization of the interior arabinan region allows for a model of the complete primary structure of *Mycobacterium tuberculosis* mycolyl arabinogalactan. *J. Biol. Chem.* **283,** 12992–13000 CrossRef Medline
16. Delmas, C., Gilleron, M., Brando, T., Vercellone, A., Gheorghiu, M., Rivière, M., and Puzo, G. (1997) Comparative structural study of the mannosylated-lipoarabinomannans from *Mycobacterium bovis* BCG vaccine strains: characterization and localization of succinates. *Glycobiology* **7,** 811–817 CrossRef Medline
17. Weber, P. L., and Gray, G. R. (1979) Structural and immunochemical characterization of the acidic arabinomannan of *Mycobacterium smegmatis*. *Carbohydr. Res.* **74,** 259–278 CrossRef Medline
18. Hunter, S. W., Gaylord, H., and Brennan, P. J. (1986) Structure and antigenicity of the phosphorylated lipopolysaccharide antigens from the leprosy and tubercle bacilli. *J. Biol. Chem.* **261,** 12345–12351 Medline
19. Torrelles, J. B., Khoo, K. H., Sieling, P. A., Modlin, R. L., Zhang, N., Marques, A. M., Treumann, A., Rithner, C. D., Brennan, P. J., and Chatterjee, D. (2004) Truncated structural variants of lipoarabinomannan in *Mycobacterium leprae* and an ethambutol-resistant strain of *Mycobacterium tuberculosis*. *J. Biol. Chem.* **279,** 41227–41239 CrossRef Medline
20. Torrelles, J. B., Sieling, P. A., Arcos, J., Knaup, R., Bartling, C., Rajaram, M. V., Stenger, S., Modlin, R. L., and Schlesinger, L. S. (2011) Structural differences in lipomannans from pathogenic and nonpathogenic mycobacteria that impact CD1b-restricted T cell responses. *J. Biol. Chem.* **286,** 35438–35446 CrossRef Medline
21. Torrelles, J. B., Sieling, P. A., Zhang, N., Keen, M. A., McNeil, M. R., Belisle, J. T., Modlin, R. L., Brennan, P. J., and Chatterjee, D. (2012) Isolation of a distinct *Mycobacterium tuberculosis* mannose-capped lipoarabinomannan isoform responsible for recognition by CD1b-restricted T cells. *Glycobiology* **22,** 1118–1127 CrossRef Medline
22. Ortalo-Magné, A., Andersen, A. B., and Daffé, M. (1996) The outermost capsular arabinomannans and other mannoconjugates of virulent and avirulent tubercle bacilli. *Microbiology* **142,** 927–935 CrossRef Medline
23. Guérardel, Y., Maes, E., Briken, V., Chirat, F., Leroy, Y., Locht, C., Strecker, G., and Kremer, L. (2003) Lipomannan and lipoarabinomannan from a clinical isolate of *Mycobacterium kansasii:* novel structural features and apoptosis-inducing properties. *J. Biol. Chem.* **278,** 36637–36651 CrossRef Medline
24. Slauch, J. M., Lee, A. A., Mahan, M. J., and Mekalanos, J. J. (1996) Molecular characterization of the oafA locus responsible for acetylation of *Salmonella typhimurium* O-antigen: OafA is a member of a family of integral membrane trans-acylases. *J. Bacteriol.* **178,** 5904–5909 CrossRef Medline
25. Thanweer, F., Tahiliani, V., Korres, H., and Verma, N. K. (2008) Topology and identification of critical residues of the *O*-acetyltransferase of serotype-converting bacteriophage, SF6, of *Shigella flexneri*. *Biochem. Biophys. Res. Commun.* **375,** 581–585 CrossRef Medline
26. Thanweer, F., and Verma, N. K. (2012) Identification of critical residues of the serotype modifying *O*-acetyltransferase of *Shigella flexneri*. *BMC Biochem.* **13,** 13 CrossRef Medline
27. Yamaryo-Botte, Y., Rainczuk, A. K., Lea-Smith, D. J., Brammananth, R., van der Peet, P. L., Meikle, P., Ralton, J. E., Rupasinghe, T. W., Williams, S. J., Coppel, R. L., Crellin, P. K., and McConville, M. J. (2015) Acetylation of trehalose mycolates is required for efficient MmpL-mediated membrane transport in Corynebacterineae. *ACS Chem. Biol.* **10,** 734–746 CrossRef Medline
28. Belardinelli, J. M., Yazidi, A., Yang, L., Fabre, L., Li, W., Jacques, B., Angala, S. K., Rouiller, I., Zgurskaya, H. I., Sygusch, J., and Jackson, M. (2016) Structure-function profile of MmpL3, the essential mycolic acid transporter from *Mycobacterium tuberculosis*. *ACS Infect. Dis.* **2,** 702–713 CrossRef Medline
29. Driessen, N. N., Stoop, E. J., Ummels, R., Gurcha, S. S., Mishra, A. K., Larrouy-Maumus, G., Nigou, J., Gilleron, M., Puzo, G., Maaskant, J. J., Sparrius, M., Besra, G. S., Bitter, W., Vandenbroucke-Grauls, C. M., and Appelmelk, B. J. (2010) *Mycobacterium marinum* MMAR_2380, a predicted transmembrane acyltransferase, is essential for the presence of the mannose cap on lipoarabinomannan. *Microbiology* **156,** 3492–3502 CrossRef Medline
30. Yamazaki, Y., Danelishvili, L., Wu, M., Macnab, M., and Bermudez, L. E. (2006) *Mycobacterium avium* genes associated with the ability to form a biofilm. *Appl. Environ. Microbiol.* **72,** 819–825 CrossRef Medline
31. Etienne, G., Villeneuve, C., Billman-Jacobe, H., Astarie-Dequeker, C., Dupont, M.-A., and Daffé, M. (2002) The impact of the absence of glycopeptidolipids on the ultrastructure, cell surface and cell wall properties, and phagocytosis of *Mycobacterium smegmatis*. *Microbiology* **148,** 3089–3100 CrossRef Medline
32. Yamazaki, Y., Danelishvili, L., Wu, M., Hidaka, E., Katsuyama, T., Stang, B., Petrofsky, M., Bildfell, R., and Bermudez, L. E. (2006) The ability to form biofilm influences Mycobacterium avium invasion and translocation of bronchial epithelial cells. *Cell Microbiol.* **8,** 806–814 CrossRef Medline
33. Rose, S. J., and Bermudez, L. E. (2014) *Mycobacterium avium* biofilm attenuates mononuclear phagocyte function by triggering hyperstimulation and apoptosis during early infection. *Infect. Immun.* **82,** 405–412 CrossRef Medline
34. Pelicic, V., Jackson, M., Reyrat, J. M., Jacobs, W. R., Jr., Gicquel, B., and Guilhot, C. (1997) Efficient allelic exchange and transposon mutagenesis in *Mycobacterium tuberculosis*. *Proc. Natl. Acad. Sci. U.S.A.* **94,** 10955–10960 CrossRef Medline
35. Grzegorzewicz, A. E., Pham, H., Gundi, V. A., Scherman, M. S., North, E. J., Hess, T., Jones, V., Gruppo, V., Born, S. E., Korduláková, J., Chavadi, S. S., Morisseau, C., Lenaerts, A. J., Lee, R. E., McNeil, M. R., and Jackson, M. (2012) Inhibition of mycolic acid transport across the *Mycobacterium tuberculosis* plasma membrane. *Nat. Chem. Biol.* **8,** 334–341 CrossRef Medline
36. Morita, Y. S., Velasquez, R., Taig, E., Waller, R. F., Patterson, J. H., Tull, D., Williams, S. J., Billman-Jacobe, H., and McConville, M. J. (2005) Compart-

mentalization of lipid biosynthesis in mycobacteria. *J. Biol. Chem.* **280,** 21645–21652 CrossRef Medline

37. Stadthagen, G., Sambou, T., Guerin, M., Barilone, N., Boudou, F., Korduláková, J., Charles, P., Alzari, P. M., Lemassu, A., Daffé, M., Puzo, G., Gicquel, B., Rivière, M., and Jackson, M. (2007) Genetic basis for the biosynthesis of methylglucose lipopolysaccharides in *Mycobacterium tuberculosis*. *J. Biol. Chem.* **282,** 27270–27276 CrossRef Medline
38. De, P., McNeil, M., Xia, M., Boot, C. M., Hesser, D. C., Denef, K., Rithner, C., Sours, T., Dobos, K. M., Hoft, D., and Chatterjee, D. (2018) Structural determinants in a glucose-containing lipopolysaccharide from *Mycobacterium tuberculosis* critical for inducing a subset of protective T cells. *J. Biol. Chem.* **293,** 9706–9717 CrossRef Medline
39. Kaur, D., McNeil, M. R., Khoo, K. H., Chatterjee, D., Crick, D. C., Jackson, M., and Brennan, P. J. (2007) New insights into the biosynthesis of mycobacterial lipomannan arising from deletion of a conserved gene. *J. Biol. Chem.* **282,** 27133–27140 CrossRef Medline
40. Berg, S., Starbuck, J., Torrelles, J. B., Vissa, V. D., Crick, D. C., Chatterjee, D., and Brennan, P. J. (2005) Roles of the conserved proline and glycosyltransferase motifs of EmbC in biosynthesis of lipoarabinomannan. *J. Biol. Chem.* **280,** 5651–5663 CrossRef Medline
41. Martin, A., Camacho, M., Portaels, F., and Palomino, J.-C. (2003) Resazurin microtiter assay plate testing of *Mycobacterium tuberculosis* susceptibilities to second-line drugs: rapid, simple, and inexpensive method. *Antimicrob. Agents Chemother.* **47,** 3616–3619 CrossRef Medline
42. Eskandarian, H. A., Odermatt, P. D., Ven, J. X. Y., Hannebelle, M. T. M., Nievergelt, A. P., Dhar, N., McKinney, J. D., and Fantner, G. E. (2017) Division site selection linked to inherited cell surface wave troughs in mycobacteria. *Nat. Microbiol.* **2,** 17094 CrossRef Medline